

## ORIGINAL ARTICLE

# Tumor-associated macrophage-derived inflammatory cytokine enhances malignant potential of malignant pleural mesothelioma

Daisuke Horio<sup>1</sup> | Toshiyuki Minami<sup>1,2</sup>  | Hidemi Kitai<sup>2</sup> | Hirotohi Ishigaki<sup>1</sup> | Yoko Higashiguchi<sup>1</sup> | Nobuyuki Kondo<sup>2,3</sup> | Seiichi Hirota<sup>4</sup> | Kazuhiro Kitajima<sup>5</sup> | Yasuhiro Nakajima<sup>1</sup> | Yuichi Koda<sup>1,2</sup> | Eriko Fujimoto<sup>1,2</sup> | Yoshiki Negi<sup>1,2</sup> | Maiko Niki<sup>1,2</sup> | Shingo Kanemura<sup>1,2</sup> | Eisuke Shibata<sup>1,2</sup> | Koji Mikami<sup>1,2</sup> | Ryo Takahashi<sup>1,2</sup> | Takashi Yokoi<sup>1,2</sup> | Kozo Kuribayashi<sup>1,2</sup> | Takashi Kijima<sup>1,2</sup>

<sup>1</sup>Department of Respiratory Medicine and Hematology, Hyogo College of Medicine, Nishinomiya, Japan

<sup>2</sup>Department of Thoracic Oncology, Hyogo College of Medicine, Nishinomiya, Japan

<sup>3</sup>Department of Thoracic Surgery, Hyogo College of Medicine, Nishinomiya, Japan

<sup>4</sup>Department of Surgical Pathology, Hyogo College of Medicine, Nishinomiya, Japan

<sup>5</sup>Division of Nuclear Medicine and PET Center, Department of Radiology, Hyogo College of Medicine, Nishinomiya, Japan

**Correspondence**

Toshiyuki Minami, Department of Respiratory Medicine and Hematology, Hyogo College of Medicine, 1-1, Mukogawa-cho, Nishinomiya, Hyogo 663-8501, Japan. Email: to-minami@hyo-med.ac.jp

**Funding information**

Japan Society for the Promotion of Science, Grant/Award Number: 18K08161, 18K15962, 18K15963 and 20K08555

**Abstract**

Malignant pleural mesothelioma (MPM) is an asbestos-related aggressive malignant neoplasm. Due to the difficulty of achieving curative surgical resection in most patients with MPM, a combination chemotherapy of cisplatin and pemetrexed has been the only approved regimen proven to improve the prognosis of MPM. However, the median overall survival time is at most 12 mo even with this regimen. There has been therefore a pressing need to develop a novel chemotherapeutic strategy to bring about a better outcome for MPM. We found that expression of interleukin-1 receptor (IL-1R) was upregulated in MPM cells compared with normal mesothelial cells. We also investigated the biological significance of the interaction between pro-inflammatory cytokine IL-1 $\beta$  and the IL-1R in MPM cells. Stimulation by IL-1 $\beta$  promoted MPM cells to form spheroids along with upregulating a cancer stem cell marker CD26. We also identified tumor-associated macrophages (TAMs) as the major source of IL-1 $\beta$  in the MPM microenvironment. Both high mobility group box 1 derived from MPM cells and the asbestos-activated inflammasome in TAMs induced the production of IL-1 $\beta$ , which resulted in enhancement of the malignant potential of MPM. We further performed immunohistochemical analysis using clinical MPM samples obtained from patients who were treated with the combination of platinum plus pemetrexed, and found that the overexpression of IL-1R tended to correlate with poor overall survival. In conclusion, the interaction between MPM cells and TAMs through a IL-1 $\beta$ /IL-1R signal could be a promising candidate as the target for novel treatment of MPM (Hyogo College of Medicine clinical trial registration number: 2973).

Daisuke Horio and Toshiyuki Minami contributed equally to this work.

This is an open access article under the terms of the Creative Commons Attribution-NonCommercial License, which permits use, distribution and reproduction in any medium, provided the original work is properly cited and is not used for commercial purposes.

© 2020 The Authors. *Cancer Science* published by John Wiley & Sons Australia, Ltd on behalf of Japanese Cancer Association.

## KEYWORDS

asbestos, IL-1 $\beta$ , inflammasome, malignant pleural mesothelioma, tumor-associated macrophage

## 1 | INTRODUCTION

Malignant pleural mesothelioma (MPM) arises from neoplastic transformation of mesothelial cells lining the pleural cavities. Epidemiological studies have proven that occupational or environmental exposure to asbestos is involved in the development of MPM and the incidence of MPM is predicted to continue increasing. Multimodal therapy including surgical treatments such as extrapleural pneumonectomy and pleurectomy/decortication is applicable only to patients with early-stage disease and good performance status.<sup>1</sup> Systemic chemotherapy with cisplatin and pemetrexed is the only approved regimen with the evidence to prolong overall survival of inoperable patients, but the median overall survival time of patients who are treated with this regimen is 12 mo after diagnosis.<sup>2,3</sup> Although recent clinical phase II studies demonstrated that nivolumab, an anti-programmed death-1 (PD-1) antibody, showed promising clinical activity in patients with relapsed MPM, there has been a lack of definitive evidence to support the practical use of nivolumab to improve the prognosis.<sup>4,5</sup> Thus, MPM still remains an aggressive and refractory malignancy which desperately calls for a novel therapeutic strategy to improve the prognosis.

Recent whole-exome sequencing analyses have identified frequent genetic alterations such as *BRCA1-associated protein 1 (BAP1)*, *p16/cyclin-dependent kinase inhibitor 2A (CDKN2A)* and *neurofibromin 2* in MPM.<sup>6</sup> Loss of BAP1 detected by immunohistochemistry and homozygous deletion of *p16* by fluorescence in situ hybridization are reliable markers for the diagnosis of MPM.<sup>7</sup> However, it is difficult to consider these MPM-causal abnormal proteins as candidates for molecular targeted therapy because they are the products not of oncogenic driver mutations but of inactivating mutations of tumor suppressor genes.<sup>8</sup>

To develop a novel molecular targeted therapy for MPM, we focused on the inflammasome in tumor-associated macrophages (TAMs). The inflammasome is collection of large multimeric danger-sensing protein complexes that promote activation of proteolytic enzyme caspase-1 (CASP1) and mediate the processing of pro-interleukin (pro-IL)-1 $\beta$  into its active form.<sup>9</sup> Recent studies have revealed that asbestos phagocytosed by macrophages triggers the formation of the inflammasome complex and promoted secretion of IL-1 $\beta$ .<sup>10,11</sup> Additionally, IL-1 $\beta$ /IL-1 receptor (IL-1R) signaling was reported to contribute to the oncogenesis of asbestos-induced mesothelioma.<sup>12</sup> These previous studies indicated the important role of the inflammasome in the development of MPM. The phagocytosed asbestos remains undegraded and induces apoptosis of macrophages.<sup>13</sup> Undegraded asbestos then undergoes phagocytosis by nearby macrophages. Thus, asbestos is not completely removed, and constitutively activates the inflammasome in macrophages. Moreover, it was reported that high mobility group box 1 (HMGB1) abundantly secreted from MPM cells and serum levels of HMGB1 are associated with poor prognosis in patients with MPM.<sup>14,15</sup> HMGB1 is one of the damage-associated molecular pattern (DAMP) proteins, and promotes pro-IL-1 $\beta$  production through functioning as

an agonist of Toll-like receptor 4 (TLR4).<sup>16</sup> TAMs serve as the major components of the tumor microenvironment, and macrophages hold the above major innate immune sensors of inflammasome and TLR4.<sup>17</sup> Therefore, we hypothesized that MPM cells and TAMs reciprocally activate one another through IL-1 $\beta$ /IL-1R signaling, not only in oncogenesis but also in disease progression.

In the present study, we investigated the interaction between MPM cells and TAMs which brought about enhancement of the malignant potential of MPM cells through IL-1 $\beta$ /IL-1R signaling.

## 2 | MATERIALS AND METHODS

### 2.1 | Cell lines and cell culture

Human MPM cell lines, MSTO-211H, H2452, H2052, and H28, and human mesothelial cell line Met-5A were obtained from the American Type Culture Collection (Manassas, VA). All these cells were cultured in RPMI 1640 medium supplemented with 10% heat-inactivated fetal bovine serum, penicillin (100 units/mL), and streptomycin (100  $\mu$ g/mL). Cells were routinely monitored for mycoplasma contamination using a Mycoplasma Detection kit (Minerva Biolabs, Berlin, Germany).

### 2.2 | Antibodies and reagents

Rabbit polyclonal antibodies (Abs) against IL-1R, and HMGB1 were purchased from abcam (Cambridge, UK) and Cell Signaling Technology (CST, Danvers, MA), respectively. Rabbit monoclonal Abs against allograft inflammatory factor-1 (AIF-1) and GAPDH were also obtained from CST. Mouse monoclonal Abs against CD26 and IL-1 $\beta$  were available from Biolegend (San Diego, CA) and CST, respectively. Functional grade mouse monoclonal Ab against IL-1 $\beta$  and its isotype control mouse IgG1 were purchased from Invitrogen (Carlsbad, CA) and used for the IL-1 $\beta$  neutralizing assay. Recombinant human IL-1 $\beta$  (rhIL-1 $\beta$ ) was purchased from PeproTech (Rocky Hill, NJ). Poly(2-hydroxyethylmethacrylate) (poly-HEMA) and phorbol 12-myristate 13-acetate (PMA) were obtained from Sigma-Aldrich (St. Louis, MO) and Wako (Osaka, Japan), respectively. Nuclear factor  $\kappa$ B (NF- $\kappa$ B) inhibitor QNZ and activator protein 1 (AP-1) inhibitor SR11302 were purchased from Selleck (Houston, TX) and R&D Systems (Minneapolis, MN), respectively.

### 2.3 | Quantitative real-time polymerase chain reaction

Total RNA from cells was extracted using an RNeasy Mini Kit (Qiagen, Valencia, CA), and cDNA was synthesized from 100 ng

total RNA using High Capacity cDNA Reverse Transcription Kits (Applied Biosystems, Waltham, MA). Quantitative real-time PCR (qRT-PCR) was performed using a SYBR Green PCR Master Mix (Applied Biosystems) on the Applied Biosystems StepOne Real-Time PCR System (Applied Biosystems) with the following profile: 1 cycle at 94°C for 2 min; 40 cycles at 94°C for 15 s, at 60°C for 1 min, and at 72°C for 1 min. Data analysis was carried out using ABI sequence detection software using relative quantification. The threshold cycle (Ct) is expressed as the mean value. The relative expression of each mRNA was calculated by the  $\Delta C_t$  method. The amount of the target gene relative to GAPDH transcripts was expressed as  $2^{-\Delta C_t}$ . Primer sequences were as follows: IL-1 $\beta$  sense: 5'-TGGCATTGATCTGGTTCATC-3', antisense: 5'-GTTTAGGAATCTCCAGTT-3', IL-1R sense: 5'-CCTGCTATGATTTCTCCAATAAA-3', antisense: 5'-CACAAAATATCACAGTCAGAGGTAGAC-3', IL-8 sense: 5'-CTGGCCGTGGCTCTCTTG-3', antisense: 5'-CCTTGGCAAACAGCACCTT-3', ALDH1A3 sense: 5'-TC TCGACAAAGCCCTGAAGT-3', antisense: 5'-TATTCGGCCAAAGC GTATTC-3', CD44 sense: 5'-AGAAGGTGTGGGCAGAAGAA-3', antisense: 5'-AAATGCACCATTTCTGAGA-3', CD26 sense: 5'-AAAATG AGTCCAAGGAAGTT-3', antisense: 5'-AAGCAGCTTGAAACTG AG-3', CASP1 sense: 5'-GCTTCTGCTCTCCACACC-3', antisense: 5'-CATCTGGCTGCTCAAATGAA-3', GAPDH sense: 5'-GCAATTC CATGGCACCGT-3', antisense: 5'-TCGCCCCACTTGATTTTGG-3'.

## 2.4 | Immunoblotting

Cells were lysed in RIPA lysis buffer (Thermo Fisher Scientific). Whole cell lysates were separated in 5%-20% gradient gel (Wako) by SDS-PAGE, and thereafter transferred to polyvinylidene difluoride membranes. The membranes were incubated with the appropriate primary Abs (diluted 1:250-500) overnight at 4°C followed by appropriate horseradish peroxidase-conjugated secondary Abs (diluted 1:1000-4000, Cell Signaling Technology) for 1 h at room temperature (RT). Immunoreactive bands were visualized using a chemiluminescence technique with Pierce ECL Plus Western Blotting Substrate (Thermo Fisher Scientific).

## 2.5 | Immunofluorescence (IF)

Cells cultured on the 12-well tissue culture plates (Corning, New York, NY) or on the bottom of Transwell plates (Corning) were fixed with 4% paraformaldehyde (Wako) for 30 min at RT. Cells were permeabilized with 0.1% Triton X-100 in phosphate-buffered saline for 5 min at RT. After being washed 3 times, cells were blocked with 1% bovine serum albumin for 60 min at RT, and were subsequently incubated with primary Abs (1:100) overnight at 4°C. For immunofluorescence detection of primary Abs, cells were washed and incubated with a 1:1000 dilution of Alexa488-labeled goat anti-mouse IgG (Thermo Fisher Scientific) for 45 min

at 4°C. Images were taken on a BZ-X700 fluorescence microscope (Keyence, Osaka, Japan).

## 2.6 | Cell proliferation assay

To assess whether rhIL-1 $\beta$  affects proliferation of H2452 cells in two-dimensional culture, H2452 cells ( $5 \times 10^3$ /well) were plated onto 96-well tissue culture-treated plates (Corning) and incubated overnight in serum-containing medium to allow the cells to attach to the plate. Then, the medium was replaced with serum-free medium, and cells were grown for up to 72 h in the presence or absence of 10 ng/mL of rhIL-1 $\beta$ . The relative number of proliferating cells was quantified every 24 h using the Cell Counting Kit-8 (CCK-8) (Dojindo, Kumamoto, Japan) following the instruction manual.

## 2.7 | Sphere formation assay

H2452 cells ( $1 \times 10^3$ /well) were plated onto poly-HEMA coated-96 well plates, and were grown in serum-free medium for 7 d with or without 10 ng/mL of rhIL-1 $\beta$  to acquire primary spheres. Then, the secondary sphere formation assay was performed to evaluate the self-renewal capacity. To generate secondary spheres, the primary spheres were collected, subsequently digested with trypsin, and resuspended in the culture medium. The numbers of secondary spheres were evaluated at day 14. During the incubation period, rhIL-1 $\beta$  was added every 3 d.

## 2.8 | Flow cytometry

To examine whether rhIL-1 $\beta$  affects the expression of CD26 on MPM cells, H2452 cells were treated with 10 ng/mL of rhIL-1 $\beta$  up to 48 h. Then, cells were detached with Accutase<sup>®</sup> (Innovative Cell Technologies, San Diego, CA), and were incubated with anti-CD26 Ab (diluted 1:100) for 45 min at 4°C followed by labeling with Alexa488-conjugated goat anti-mouse IgG (Thermo Fisher Scientific). After staining, cells were analyzed by BD LSRFortessa (Becton Dickinson, Franklin Lakes, NJ).

## 2.9 | Signal transduction analysis

To determine the signal transduction pathway of CD26 induction by rhIL-1 $\beta$ , H2452 cells were plated onto 6-well plates (Iwaki, Haibara, Japan) and were preincubated overnight in serum-free medium containing either DMSO, 100 nmol/L of QNZ or 10  $\mu$ mol/L of SR11302 as previously described.<sup>18,19</sup> Thereafter, cells were stimulated with 10 ng/mL of rhIL-1 $\beta$  for 8 h, and lysed to extract total RNA. The amount of CD26 transcripts was measured by qRT-PCR.

## 2.10 | Knock down (KD) analysis

For CD26 KD analysis, H2452 cells were grown in 12-well tissue culture-treated plates (Corning, New York, NY) and transfected with either 20 pmol/L of small interfering RNA (siRNA) targeted CD26 (Silencer<sup>®</sup> Select, s4254 as #1 and s4255 as #2, Ambion, Austin, TX), or control siRNA (Silencer<sup>®</sup> Select, Negative Control #1) using Lipofectamine RNAiMAX (Invitrogen). For CASP1 KD analysis, THP-1 cells were grown in 12-well tissue culture-treated plates (Corning) and transfected with either 100 pmol/L of small interfering RNA (siRNA) targeted CASP1 (Silencer<sup>®</sup> Select, s2407) using Viromer<sup>®</sup> GREEN (Lipocalyx, Weinbergweg, Germany). After 48 h, cells were harvested and used for the individual experiments.

## 2.11 | Coincubation assay

Coincubation assay was performed as previously described.<sup>20,21</sup> Briefly, the day before starting coincubation, H2452 cells ( $3 \times 10^4$ /well) and THP-1 cells ( $5 \times 10^4$ /well) were seeded separately onto 12-well tissue culture plates and 12-well Transwell inserts with a 0.4  $\mu$ m pore size (Costar). THP-1 cells were differentiated to macrophages using 320 nmol/L PMA. Thereafter, the inserts containing THP-1-derived macrophages were placed on the well that was culturing H2452 cells. At 5 d after starting coincubation, the culture medium was harvested to perform enzyme-linked immunosorbent assay (ELISA), then both THP-1-derived macrophages and H2452 cells were lysed to extract total RNA. In another experiment, H2452 cells were also used for IF analysis.

## 2.12 | ELISA

After 5 d coincubation of H2452 cells and THP-1-derived macrophages, the supernatants from each well were collected, and the concentration of human IL-1 $\beta$  was measured using Quantikine kits (R&D Systems) according to the manufacturer's protocol.

## 2.13 | Clinical MPM tissue samples

Malignant pleural mesothelioma tissue samples were collected from the patients diagnosed with MPM by surgical biopsy at Hyogo College of Medicine Hospital (Nishinomiya, Japan) from August 2017 to September 2018. This study was approved by the institutional review board of Hyogo College of Medicine (Trial number: 2973), and all the patients provided written informed consent.

## 2.14 | Immunohistochemistry (IHC)

Next, 4- $\mu$ m thick sections were deparaffinized and incubated in Target Retrieval Solution pH 9.0 (Agilent, Santa Clara, CA) for 40 min

at 96°C for antigen retrieval, then endogenous peroxidase activity and nonspecific antibody binding were blocked with peroxidase blocking solution (Agilent) and normal goat serum, respectively. The sections were allowed to react with diluted anti-IL-1R rabbit polyclonal Ab (1:500) or anti-AIF-1 rabbit monoclonal Ab (1:500) overnight. Then, the slides were incubated with a peroxidase-labeled polymer conjugated to a secondary anti-rabbit Ab using EnVision FLEX/HRP (Agilent) and developed with 3,3'-deaminobenzidine as the chromogen.

Immunoreactiveness for IL-1R expression was scored by immunoreactive score (IRS) as previously described.<sup>22</sup> Briefly, IRS (values from 0 to 12) is calculated as a product of multiplication between immunostaining intensity (ISI: 0 = absent; 1 = weak; 2 = moderate; 3 = strong) and proportion score (PS: 0 = no positive cells; 1 = < 10% of positive cells; 2 = 10%-50% of positive cells; 3 = 51%-80% of positive cells; 4 = 80% of positive cells). Positive cells were quantified using Hybrid Cell Count software BZ-H3C (Keyence).

## 2.15 | Statistical analysis

All the in vitro studies for statistical evaluation were performed in triplicate in each experiment and repeated at least 3 times. Mean  $\pm$  SEM values were calculated and differences were evaluated by two-sided Student *t* test. *P* < .05 values were considered statistically significant.

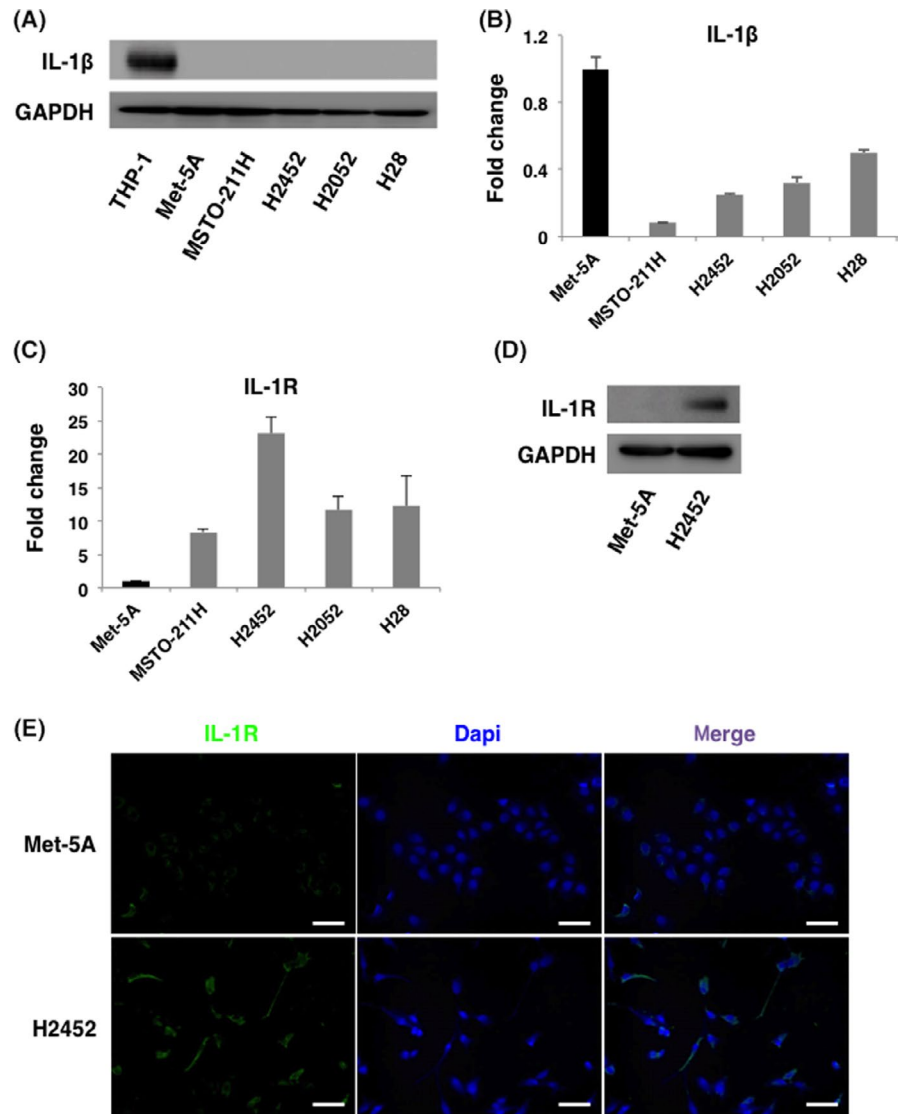
Progression-free survival (PFS) and overall survival (OS) were calculated using the Kaplan-Meier method from the date of chemotherapy initiation to the date of recurrence and from the date of initial diagnosis to the date of death, respectively. Survival curves were compared using log-rank testing.

# 3 | RESULTS

## 3.1 | IL-1R is overexpressed in MPM cells

To investigate the role of inflammatory cytokine IL-1 $\beta$  in the disease progression of MPM, we first evaluated the expression of IL-1 $\beta$  protein and transcripts by qRT-PCR in human mesothelial cell (Met-5A), and MPM cells (MSTO-211H, H2452, H2052, and H28). Immunoblotting analysis showed that IL-1 $\beta$  protein was not expressed at any detectable levels in both Met-5A cells and MPM cells (Figure 1A). Moreover, the amount of IL-1 $\beta$  transcripts was lower in all 4 MPM cell lines than Met-5A cells (Figure 1B). Based on these results, IL-1 $\beta$  expression was considered to be extremely low in MPM cells. In contrast, expression of IL-1R, a receptor for IL-1 $\beta$ , was higher in MPM cells than in Met-5A cells (Figure 1C). Immunoblotting and IF analyses performed on Met-5A cells and H2452 cells also demonstrated the enhancement of IL-1R expression in MPM cells at the protein level (Figure 1D,E). These results indicated that the amount of IL-1R expression is independent of endogenous IL-1 $\beta$  expression in normal mesothelial cells and MPM cells.

**FIGURE 1** IL-1R is overexpressed in malignant pleural mesothelioma (MPM) cells compared with mesothelial cells. A, Comprehensive analysis of IL-1 $\beta$  expression in human mesothelial cell (Met-5A) and MPM cell lines (MSTO-211H, H2452, H2052, and H28) by immunoblotting. Cell lysates from THP-1 cells were loaded as a positive control. Expression of IL-1 $\beta$  was detected neither in mesothelial cell nor in MPM cells. B, Comprehensive analysis of IL-1 $\beta$  expression in human mesothelial cell and MPM cell lines by qRT-PCR. Expression of IL-1 $\beta$  transcripts was less in all the MPM cells than in mesothelial cells. C, Comprehensive analysis of IL-1R expression in human mesothelial cells and MPM cells lines by qRT-PCR. Expression of IL-1R was higher in MPM cells than in mesothelial cells. D, E, Protein level of IL-1R in human mesothelial cell (Met-5A) and MPM cell (H2452) was examined by immunoblotting and immunofluorescence. Consistent with the results of qRT-PCR and immunoblotting, expression of IL-1R was higher in H2452 cells. All the above experiments were performed at least twice with similar results. Representative data are shown. Scale Bars, 100  $\mu$ m



### 3.2 | IL-1 $\beta$ promotes sphere formation through upregulation of CD26 in MPM cells

We then examined the biological effect of IL-1 $\beta$  on MPM cells. First, we measured the expression of IL-8, which is a well known IL-1 $\beta$ -inducible gene, at the transcript level.<sup>23</sup> H2452 cells, which showed the highest expression of IL-1R among the 4 MPM cell lines, most dramatically induced IL-8 transcription in response to rhIL-1 $\beta$  stimulation (Figure S1). These results suggested that the signal intensity of IL-1 $\beta$ /IL-1R axis was dependent on the amount of IL-1R expression in MPM cells. Next, we performed two-dimensional (2D) cell proliferation assay and three-dimensional sphere formation assay to elucidate the biological activity of rhIL-1 $\beta$  on H2452 cells. Although rhIL-1 $\beta$  did not affect cell proliferation in 2D culture (Figure S2), the number of secondary spheroids significantly increased in the presence of rhIL-1 $\beta$  in H2452 cells (Figure 2A), indicating that rhIL-1 $\beta$  enhanced self-renewal capacity of MPM cells. We then assessed the expression of ALDH1A3, CD44, and CD26. ALDH1A3 and CD44 were widely recognized and CD26 was recently identified as a

cancer stem cell (CSC) marker of MPM.<sup>24-26</sup> The expression levels of the transcripts of these CSC markers were similarly increased by rhIL-1 $\beta$  stimulation (Figure 2B). Among these CSC markers, we focused on CD26, which has been recently reported to be clinically actionable by a novel monoclonal antibody, YS-110.<sup>27</sup> Consistent with the results for the transcripts, flow cytometry analysis demonstrated that cell surface CD26 expression was upregulated in a time-dependent manner by rhIL-1 $\beta$  stimulation (Figure 2C). We further investigated the pathway involved in rhIL-1 $\beta$ -induced CD26 upregulation. Transcription factors NF- $\kappa$ B and AP-1 are downstream signaling molecules of the IL-1 $\beta$ /IL-1R axis.<sup>28</sup> As shown in Figure 2D, rhIL-1 $\beta$ -induced CD26 upregulation was significantly inhibited by AP-1 inhibitor SR11302 but not by NF- $\kappa$ B inhibitor QNZ. This result indicated that rhIL-1 $\beta$  induced CD26 expression via activation of AP-1.

To determine the involvement of CD26 in self-renewal capacity, we knocked down CD26 by transfecting 1 of 2 siRNAs of different sequences (siCD26 #1 or siCD26 #2) in H2452 cells (Figure S3). Sphere formation assay demonstrated that the number of spheroids

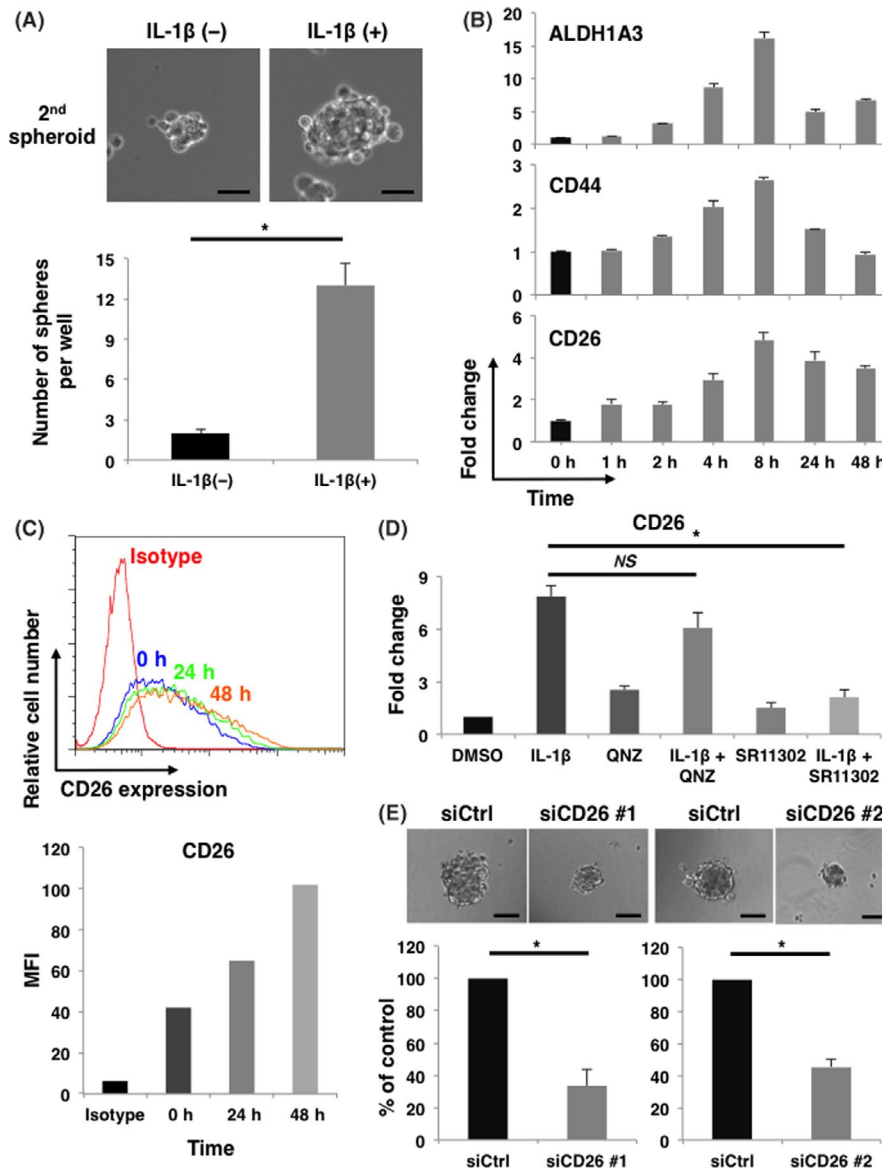


**FIGURE 2** IL-1 $\beta$  promotes sphere formation through upregulation of CD26 in IL-1R-overexpressing H2452 cells. A, H2452 cells were cultured with or without 10 ng/mL of rhIL-1 $\beta$  on poly-HEMA plate to evaluate sphere forming ability. Representative phase contrast images and quantification of the number of spheres are shown in upper and lower panel, respectively. Results represent the mean  $\pm$  SEM of 3 independent experiments performed in triplicates. Scale bars, 50  $\mu$ m, \* $P$  < .01. B, Representative data of expression of ALDH1A3, CD44, and CD26 transcripts induced by rhIL-1 $\beta$  at the indicated time points are shown. Experiments were repeated twice in triplicates with similar results. Error bars, SEM. C, Cell surface CD26 expression induced by 10 ng/mL of rhIL-1 $\beta$  at the indicated time points was analyzed by flow cytometry. Representative histogram and mean fluorescence intensity (MFI) are shown in upper and lower panel, respectively. Experiments were repeated twice with similar results. Error bars, SEM. D, Expression of CD26 transcripts in H2452 cells stimulated by 10 ng/mL of rhIL-1 $\beta$  for 8 h in the presence of QNZ or SR11302 was measured by qRT-PCR. Results represent mean  $\pm$  SEM of 3 independent experiments performed in triplicates. \* $P$  < .01. E, Sphere forming ability of H2452 cells either transfected with control or 2 different CD26 targeting siRNAs (siCD26 #1 and siCD26 #2) was examined. Representative phase contrast images and quantification of the relative number of spheres are shown in left and right panel, respectively. Results represent mean  $\pm$  SEM of 3 independent experiments performed in triplicates. Scale bars, 100  $\mu$ m, \* $P$  < .01.

significantly decreased in both CD26 targeting siRNAs (siCD26 #1 and siCD26 #2)-transfected H2452 cells compared with control siRNA-transfected H2452 cells (Figure 2E). These results demonstrated that IL-1 $\beta$  functions as a paracrine mediator, enhancing the acquisition of CSC-like phenotype in MPM cells via the upregulation of CD26.

### 3.3 | IL-1 $\beta$ derived from macrophages induces CD26 expression in MPM cells

As MPM cells produced low levels of IL-1 $\beta$  (Figure 1A,B), we presumed that macrophages such as TAMs, the major components of tumor microenvironment, are the most expected source of IL-1 $\beta$ . To

determine the interaction between MPM cells and macrophages, we then coincubated H2452 cells and THP-1-derived macrophages, as shown in Figure . Quantitative RT-PCR analysis revealed that coincubation with H2452 cells enhanced both arginase-1 (ARG1) and inducible nitric oxide synthesis (iNOS) transcription in THP-1-derived macrophages. Notably, transcription of Arg-1 was preferentially

induced compared with that of iNOS (Figure 3B). These results suggested that THP-1-derived macrophages coincubated with H2452 cells were activated and relatively polarized toward alternative M2 forms of activation characterized as TAMs.

Expression of IL-1 $\beta$  transcripts in THP-1-derived macrophages was significantly increased when coincubated with H2452 cells.

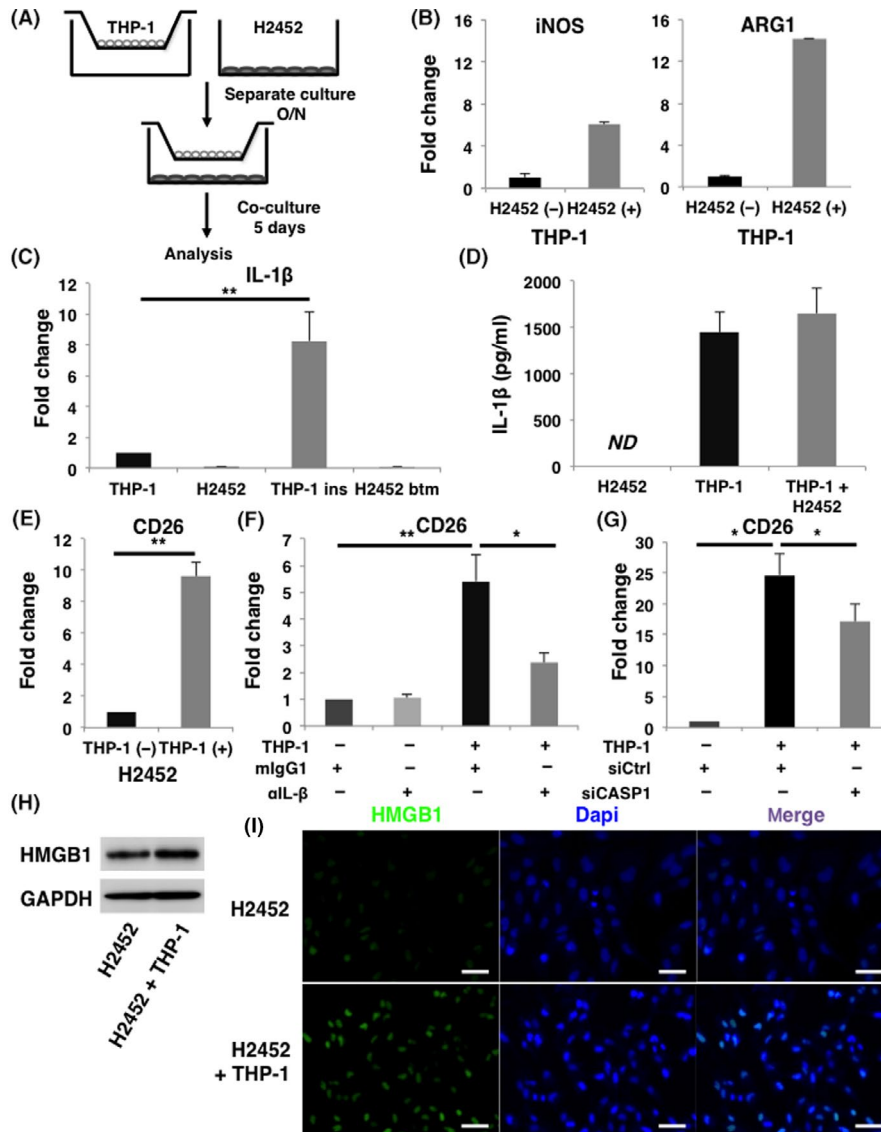


**FIGURE 3** IL-1 $\beta$  derived from macrophages induces CD26 expression in malignant pleural mesothelioma (MPM) cells. A, Schema of coincubation assay. THP-1-derived macrophages and H2452 cells were coincubated for 5 d and separately analyzed. B, Expression of transcripts of M1 marker iNOS and M2 marker ARG1 in THP-1-derived macrophages in the absence or presence of coincubating with H2452 cells are shown in the left and right panels, respectively. C, Amounts of IL-1 $\beta$  transcripts in H2452 cells and THP-1-derived macrophages were measured by qRT-PCR. Results of the samples of THP-1-derived macrophages in the insert (THP-1 ins) and H2452 cells in the bottom well (H2452 btm) harvested after coincubation using Transwell (Costar) inserts were presented in the third and fourth lane from the left, respectively. D, ELISA analysis about the concentration of IL-1 $\beta$  in the culture medium. Samples were collected from the supernatants of H2452 cells, THP-1-derived macrophages, and co-culture medium of these cells. ND, not detected. E, Amount of CD26 transcripts in H2452 cells under coincubation with THP-1-derived macrophages was also analyzed by qRT-PCR. F, Expression of CD26 transcripts in H2452 cells when coincubated with THP-1-derived macrophage in the presence of 1  $\mu$ g/mL of anti-IL-1 $\beta$  neutralizing Ab ( $\alpha$ IL-1 $\beta$ ) or its isotype control mouse IgG1 (mIgG1) was evaluated. G, CD26 gene expression in H2452 cells was examined when coincubated with either control or CASP1 siRNA-transfected THP-1-derived macrophages. H, Expression of HMGB1 in H2452 cells under coincubation with THP-1-derived macrophages was examined by immunoblotting. I, Representative immunofluorescence images are shown of HMGB1 expression in H2452 cells when they were coincubated with THP-1-derived macrophages. All the experiments were performed at least 3 times. Quantification data represent mean  $\pm$  SEM. \* $P$  < .05, \*\* $P$  < .01, Scale bars, 50  $\mu$ m

Conversely, low expression levels of IL-1 $\beta$  transcripts were detected in H2452 cells, even though they were cocubated with THP-1-derived macrophages (Figure 3C). ELISA revealed that large amounts of IL-1 $\beta$  remained in the culture medium when THP-1-derived macrophages were cocubated with H2452 cells, regardless of being taken up by internalization after binding with IL-1R (Figure 3D). These results suggested that cocubation with THP-1-derived macrophages and H2452 cells induced IL-1 $\beta$  secretion from THP-1-derived macrophages. Simultaneously, expression of CD26 transcripts in H2452 cells was upregulated by coculturing with THP-1-derived macrophages (Figure 3E). This phenomenon of upregulation of CD26 transcripts in H2452 cells was significantly blocked by adding anti-IL-1 $\beta$  neutralizing antibody to the co-culture medium (Figure 3F).

To clarify the role of inflammasome in macrophages, we knocked down CASP1 in THP-1-derived macrophages (Figure S4). The concentration of IL-1 $\beta$  in co-culture medium was markedly decreased (Figure S5). Consequently, cocubation-induced upregulation of CD26 expression in H2452 cells was significantly attenuated when they were cocubated with CASP1-KD THP-1-derived macrophages (Figure 3G). These results indicated that IL-1 $\beta$  activated by the inflammasome in macrophages was involved in promoting the feature MPM cells to acquire the more aggressive CSC-like phenotype. Furthermore, protein levels of HMGB1 in H2452 cells were enhanced when cells were cocubated with THP-1-derived macrophages, despite the marginal increase in transcript level (Figures 3H,I; S6). Thus, MPM cells acquired CSC-like properties as a result of interaction with TAMs.

### 3.4 | Overexpression of IL-1R tends to be associated with poor overall survival in patients with MPM treated with combination therapy of platinum plus pemetrexed

To investigate the clinical significance of IL-1R expression in MPM, immunoreactivity for IL-1R expression was assessed by IHC on 21 human MPM samples collected from patients who were treated with platinum plus pemetrexed combination therapy. The patients' clinicopathologic characteristics are shown in Table 1. The most common histological subtypes were epithelioid ( $n = 16$ , 76.2%), and about half of the patients ( $n = 10$ , 47.6%) were diagnosed at an early stage (stage I or stage II). As shown in Figure 4A, various levels of ISI for IL-1R expression were observed in MPM clinical samples. In these samples, low IRS (score: 0-3), low-intermediate IRS (score: 4, 6), high-intermediate IRS (score: 8, 9), high IRS (score: 12) was observed in 4, 7, 5, and 5 samples, respectively, and the median IRS was 6 (Table S1). According to the median IRS value of 6, we classified MPM samples into 2 groups and compared the survival curves of PFS and OS between the IRS low (score: 0-6) group and the IRS high (score: 8-12) group. The median PFS was 161 and 110 d in the IRS low group and IRS high group, respectively (Figure 4B). The median OS in the IRS low group was 407 d and tended to be longer than the 237 d of the IRS high group (Figure 4C). As a result, there was no statistically significant difference between the 2 groups with

**TABLE 1** Clinicopathological characteristics of the enrolled patients

Characteristics	
Total number	21
Gender	
Male	20
Female	1
Age, $y \pm SD$	$70.1 \pm 6.3$
Asbestos exposure	
Occupational	14
Environmental	3
Unknown	4
Histological type	
Epithelioid	16 (76.2%)
Biphasic	2 (9.5%)
Sarcomatoid	3 (14.3%)
Stage	
I	7
II	3
III	6
IV	5
2nd line chemotherapy	
Nivolumab	9
None	12

Abbreviation: SD, standard deviation.

respect to PFS and OS. Disease control rate seemed to be slightly worse in the IRS high group but no significant difference was observed between these 2 groups (Table 2). These results suggested that overexpression of IL-1R could be a negative prognostic factor in patients who were treated with a standard chemotherapeutic regimen of platinum plus pemetrexed. We further performed IHC analysis to evaluate activated TAMs in these MPM samples by staining for AIF-1, which is commonly recognized as a marker of activated macrophages.<sup>29</sup> Although statistically significant correlation between IL-1R IRS and AIF-positive cell ratio was not observed (Figure 4D), TAMs abundantly infiltrated into every histological type of MPM tissues (Figure 4E). These results implied the substantial role of TAMs in the progression of MPM.

## 4 | DISCUSSION

Based on the epidemiological and experimental studies, asbestos is proven to be involved in the development of MPM.<sup>10,30</sup> However, it remains unknown whether asbestos is related to the progression of MPM. Asbestos has been reported to activate the inflammasome, which functions as a key modulator in the processing of pro-IL-1 $\beta$ .<sup>9</sup> In the present study, we demonstrated that IL-1 $\beta$  secreted from TAMs contributes to promoting the malignant potential of MPM cells via interaction with IL-1R.

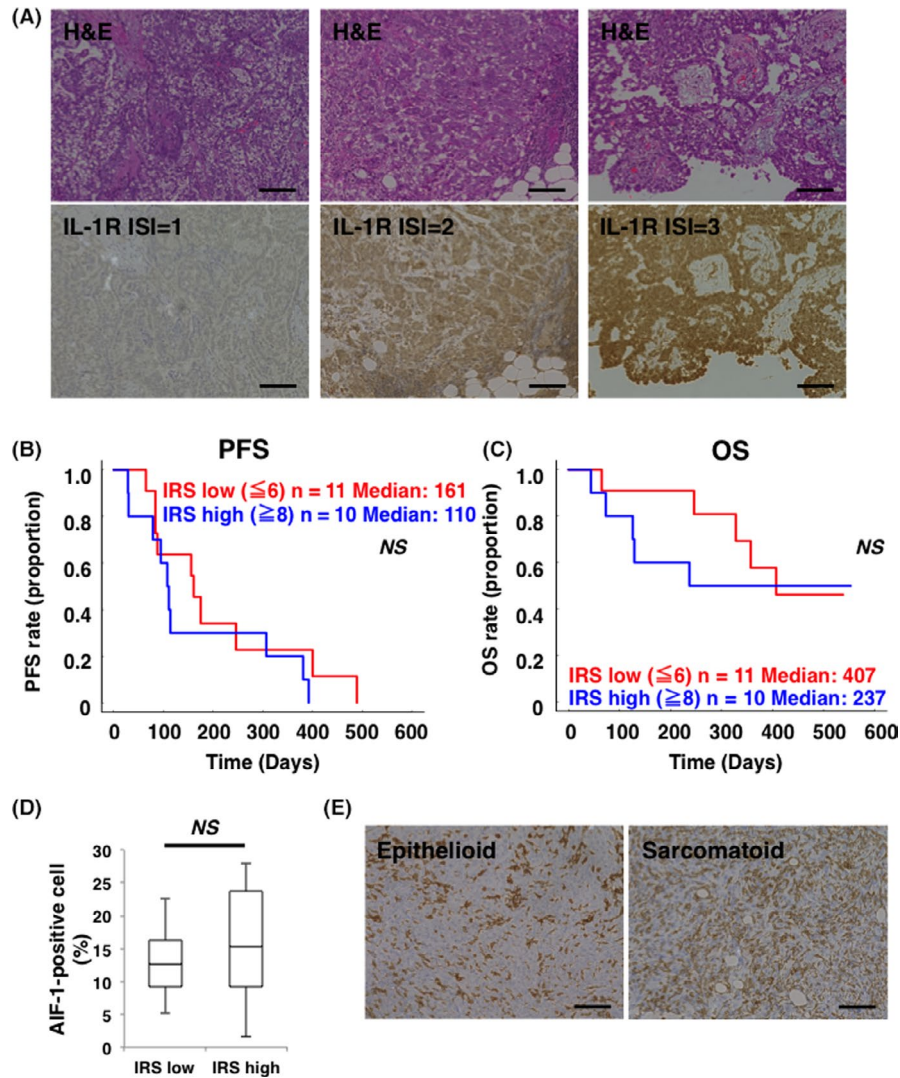


**FIGURE 4** Overexpression of IL-1R may be a negative prognostic factor in patients with malignant pleural mesothelioma (MPM) who were treated with platinum plus pemetrexed. A, Representative images of hematoxylin-eosin staining and IL-1R IHC staining of clinical samples from patients with MPM are shown in the upper panels and lower panels, respectively. Immunostaining intensity (ISI) for IL-1R was scored from negative to strong. Mild staining (ISI = 1), moderate staining (ISI = 2), and strong staining (ISI = 3) were indicated in lower left, center, and right panel, respectively. Scale bars, 100  $\mu$ m. B, Kaplan-Meier curve for progression-free survival (PFS) between the immunoreactive score (IRS) low group (n = 11, red) and the high group (n = 10, blue). C, Kaplan-Meier curve for OS between IRS score low group (n = 11, red) and high group (n = 10, blue). NS, not significant. D, Comparison of AIF-1-positive cell ratio in MPM tissue between the IRS low group (n = 11) and IRS high group (n = 10). The middle line, the upper end, and the lower end of the box plot represent median, 75% and 25% values, respectively. NS, not significant. E, Representative images of AIF-1 immunohistochemistry (IHC) staining of epithelioid and sarcomatoid MPM samples were shown in the left panel and right panel, respectively. Scale bars, 100  $\mu$ m

**TABLE 2** Response to combination therapy of platinum plus pemetrexed in accordance with IRS of IL-1R expression

IL-1R IRS	CR	PR	SD	PD	DCR (%)
Low	0	3	5	3	72.7
High	0	2	4	4	60.0
Total	0	5	9	7	66.7

Abbreviation: CR, complete response; DCR, disease control rate.; IRS, immunoreactive score; PD, progressive disease; PR, partial response; SD, stable disease.

One of the reasons for the poor prognosis in MPM is the

refractiveness to systemic chemotherapy. Even though the tumor responds to systemic chemotherapy and shrinks, it easily recurs and regrows. To elucidate the mechanism of the refractiveness to chemotherapy in MPM, we examined whether IL-1 $\beta$  played a key role for MPM cells to acquire a CSC-like phenotype. We demonstrated that exogenous IL-1 $\beta$  stimulation promoted spheroid formation along with CD26 upregulation (Figure 2A-C). CD26 is a transmembrane glycoprotein with dipeptidyl peptidase 4 activity, and had originally been described as a T-cell activation molecule.<sup>31</sup> Recent studies have demonstrated that CD26 is expressed not only on T cells but also on various types of tumors including MPM.<sup>32</sup> CD26 was also identified as a CSC marker especially in MPM and colorectal

cancer.<sup>25,26,33</sup> Indeed, sphere formation assay showed that self-renewal capacity significantly decreased following CD26-KD in H2452 cells (Figure 2E). These results indicated that IL-1 $\beta$  contributed to the acquisition of a CSC-like phenotype via CD26 upregulation.

Despite the overexpression of IL-1R, MPM cells were found to produce low levels of IL-1 $\beta$ , which played a huge role in the promotion of sphere formation (Figure 1A,B). Therefore, we presumed that IL-1 $\beta$  would affect MPM cells mainly via the paracrine mechanism. Regarding the source of IL-1 $\beta$ , we focused on TAMs. It has been reported that the macrophages activated by engulfing asbestos played a pivotal role in the oncogenesis of MPM by causing a chronic inflammatory response.<sup>34</sup> In particular, IL-1 $\beta$  has been shown to be linked to asbestos-induced oncogenesis among various kinds of macrophage-derived inflammatory cytokines.<sup>10,12</sup> However, it has remained unknown whether IL-1 $\beta$  is involved in disease progression as well as oncogenesis in MPM. Coincubation assay of THP-1-derived macrophages and MPM cells revealed that macrophages were polarized toward the M2 phenotype, which is known as a pro-tumorigenic feature of TAMs,<sup>35</sup> and the reinforcement of malignant potential were suggested by the evidence of CD26 upregulation in MPM cells (Figure 3B,E). Moreover, as we show in Figure 3H,I and Figure S6, macrophages may prevent HMGB1 from undergoing proteolytic degradation in MPM cells. HMGB1 interacts with TLR4 and promotes the production of pro-IL-1 $\beta$ ,<sup>16</sup> possibly a reason why higher levels of HMGB1 are associated with poor outcome in patients with MPM, as we previously described.<sup>15</sup>

We summarize the relationship between TAMs and MPM cells in Figure 5. HMGB1 released from MPM cells (signal 1) induces pro-IL-1 $\beta$  production through interactions with TLR4 in TAMs. In TAMs, phagocytosed asbestos constitutively activates the inflammasome (signal 2), which causes maturation and secretion of IL-1 $\beta$ . Secreted IL-1 $\beta$  interacts with IL-1R on MPM cells via a paracrine mechanism. Finally, MPM cells acquire a CSC-like phenotype.

A recent clinical study using human MPM samples demonstrated that higher levels of macrophages in tumor microenvironment were associated with aggressive histopathological features.<sup>36</sup> Furthermore, IHC results presented in Figure 4C indicated that overexpression of IL-1R on MPM cells might be a negative prognostic factor. Notably, IL-1R overexpression seemed to be more closely correlated with OS rather than PFS in MPM patients who received standard chemotherapy. Regarding the reason why OS was strongly influenced by the amount of IL-1R expression compared with PFS, we speculate as follows. Cytotoxic chemotherapy can induce apoptotic cell death in tumor cells, which cause the extracellular release of HMGB1.<sup>37</sup> HMGB1 promotes the secretion of IL-1 $\beta$  from TAMs through interacting with their TLR4. IL-1 $\beta$  encourages MPM cells to acquire CSC potential through interacting with IL-1R. Generally, these cells harboring CSC properties are difficult to eliminate but are quiescent and exhibit longer doubling time,<sup>38</sup> which after all might bring about shorter OS and longer PFS in patients with IL-1R-overexpressing MPM. These results and perspectives clinically highlighted the importance of the interaction between

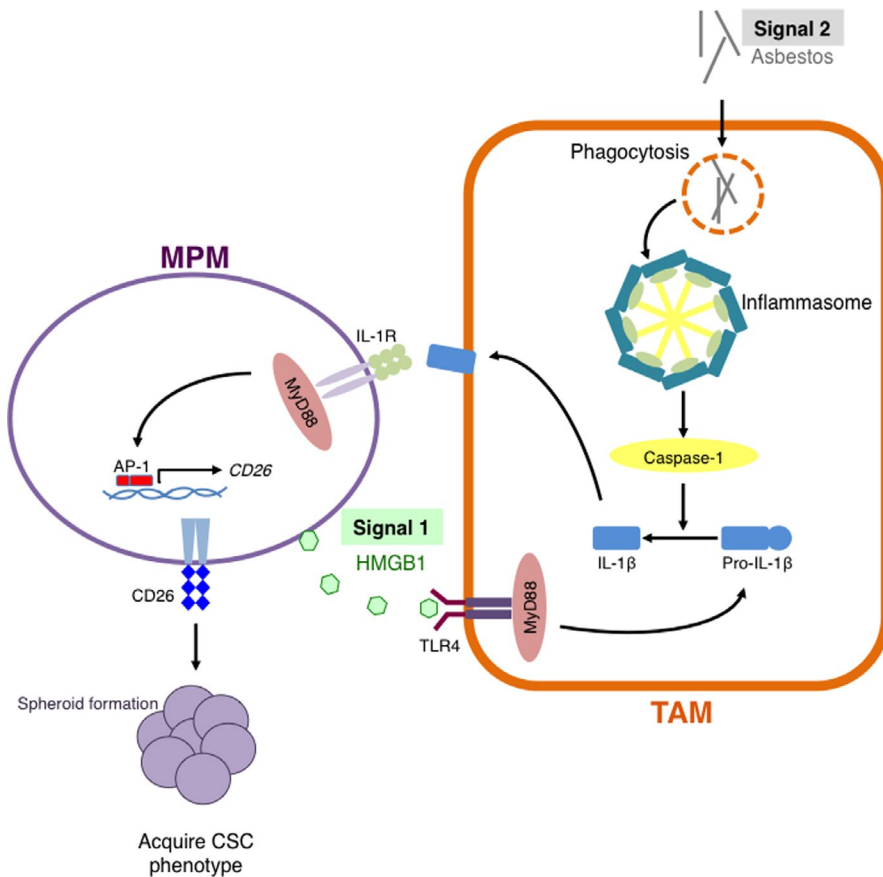


**FIGURE 5** Tumor-associated macrophages (TAMs) contribute in the acquisition of a CSC-like phenotype in malignant pleural mesothelioma (MPM) cells via IL-1 $\beta$ /IL-1R axis. HMGB1 released from MPM cells (signal 1) induces pro-IL-1 $\beta$  production through activating TLR4 in TAMs. In TAMs, phagocytosed asbestos constitutively activates the inflammasome (signal 2), which in turn causes maturation and secretion of IL-1 $\beta$ . Secreted IL-1 $\beta$  interacts with IL-1R on MPM cells via a paracrine mechanism. Finally, MPM cells acquire a cancer stem cell (CSC)-like phenotype

TAMs and MPM cells through IL-1 $\beta$ /IL-1R axis in the disease progression of MPM.

From translational points of views, anti-CD26 antibody YS-110 and anti-IL-1 $\beta$  antibody canakinumab are considered to be promising candidates for the novel treatment of MPM. YS-110 was reported to exert antitumor effect against MPM cells through inducing antibody-dependent cell-mediated cytotoxicity and cell cycle arrest via p27<sup>kip1</sup> accumulation.<sup>39</sup> According to the results of phase I clinical trial, YS-110 therapy was well tolerable and showed durable effect for some patients with MPM.<sup>27,40</sup> A phase II study to evaluate antitumor effect for the treatment of MPM is now ongoing. Canakinumab was originally approved for the treatment of patients with chronic inflammatory disease including cryopyrin-associated periodic syndrome, juvenile idiopathic arthritis, and refractory gout.<sup>41</sup> Interestingly, it was reported that canakinumab reduced the incidence of lung cancer in patients with atherosclerosis.<sup>42</sup> Although there has been no preclinical or clinical data that have demonstrated the antitumor activity of canakinumab in MPM, our data indicated that canakinumab may prevent MPM cells from acquiring a CSC-like phenotype. Conversely, as a currently approved drug, we consider that nivolumab can eliminate CSC-like MPM cells. Recent preclinical study also demonstrated that PD-1 expression in TAMs negatively correlated with their phagocytic activity and anti-PD-1 antibody could increase macrophage phagocytosis and reduce tumor growth.<sup>43</sup> Indeed, as shown in Figure 4C, the survival curve reached a plateau even in the patients with a high IL-1R IRS score, and 4 of 5 patients who survived for more than 1 y in the IRS high group were found to have received nivolumab monotherapy as 2nd line chemotherapy. Additionally, the OS curve in Figure S7 demonstrated the marked improvement in the outcome of the patients who were able to receive nivolumab monotherapy. These clinical findings indicated that nivolumab has the potential to bring about a better prognosis to the patients with MPM regardless of IL-1R expression. Thus, YS-110, canakinumab, and nivolumab are expected to overcome MPM cells with a CSC-like phenotype via their respective mechanisms.

In conclusion, TAMs play a critical role in the disease progression of MPM, and targeting the interaction between TAMs and MPM cells via IL-1 $\beta$ /IL-1R axis is a promising, novel therapeutic strategy in patients with MPM.

#### ACKNOWLEDGMENTS

This work was supported by Grant-in-Aid for Scientific Research from the Ministry of Education, Culture, Sports, Science and Technology, Japan (18K15962 and 20K08555 to TM, 18K15963 to SK, 18K08161 to TK).

#### DISCLOSURE

No potential conflicts of interest were disclosed.

#### ORCID

Toshiyuki Minami  <https://orcid.org/0000-0001-7421-8457>

#### REFERENCES

- Ricciardi S, Cardillo G, Zirafa CC, et al. Surgery for malignant pleural mesothelioma: an international guidelines review. *J Thorac Dis.* 2018;10(Suppl 2):S285-S292.
- Scherpereel A, Wallyn F, Albelda SM, Munck C. Novel therapies for malignant pleural mesothelioma. *Lancet Oncol.* 2018;19(3):e161-e172.
- Bibby AC, Tsim S, Kanellakis N, et al. Malignant pleural mesothelioma: an update on investigation, diagnosis and treatment. *Eur Respir Rev.* 2016;25(142):472-486.
- Quispel-Janssen J, van der Noort V, de Vries JF, et al. Programmed death 1 blockade with nivolumab in patients with recurrent malignant pleural mesothelioma. *J Thorac Oncol.* 2018;13(10):1569-1576.
- Scherpereel A, Mazieres J, Greillier L, et al. Nivolumab or nivolumab plus ipilimumab in patients with relapsed malignant pleural mesothelioma (IFCT-1501 MAPS2): a multicentre, open-label, randomised, non-comparative, phase 2 trial. *Lancet Oncol.* 2019;20(2):239-253.
- Guo G, Chmielecki J, Goparaju C, et al. Whole-exome sequencing reveals frequent genetic alterations in BAP1, NF2, CDKN2A, and CUL1 in malignant pleural mesothelioma. *Cancer Res.* 2015;75(2):264-269.
- Hwang HC, Pyott S, Rodriguez S, et al. BAP1 Immunohistochemistry and p16 FISH in the diagnosis of sarcomatous and desmoplastic mesotheliomas. *Am J Surg Pathol.* 2016;40(5):714-718.
- Hylebos M, Van Camp G, van Meerbeeck JP, Op de Beeck K. The genetic landscape of malignant pleural mesothelioma: results from massively parallel sequencing. *J Thorac Oncol.* 2016;11(10):1615-1626.
- Wen H, Ting JP, O'Neill LA. A role for the NLRP3 inflammasome in metabolic diseases—did Warburg miss inflammation? *Nat Immunol.* 2012;13(4):352-357.
- Carbone M, Yang H. Molecular pathways: targeting mechanisms of asbestos and erionite carcinogenesis in mesothelioma. *Clin Cancer Res.* 2012;18(3):598-604.
- Sayan M, Mossman BT. The NLRP3 inflammasome in pathogenic particle and fibre-associated lung inflammation and diseases. *Part Fibre Toxicol.* 2016;13(1):51.
- Kadariya Y, Menges CW, Talarchek J, et al. Inflammation-related IL1 $\beta$ /IL1R signaling promotes the development of asbestos-induced malignant mesothelioma. *Cancer Prev Res (Phila).* 2016;9(5):406-414.
- Hamilton RF, Iyer LL, Holian A. Asbestos induces apoptosis in human alveolar macrophages. *Am J Physiol.* 1996;271(5 Pt 1):L813-L819.
- Jube S, Rivera ZS, Bianchi ME, et al. Cancer cell secretion of the DAMP protein HMGB1 supports progression in malignant mesothelioma. *Cancer Res.* 2012;72(13):3290-3301.
- Tabata C, Shibata E, Tabata R, et al. Serum HMGB1 as a prognostic marker for malignant pleural mesothelioma. *BMC Cancer.* 2013;13:205.
- Maroso M, Balosso S, Ravizza T, et al. Toll-like receptor 4 and high-mobility group box-1 are involved in ictogenesis and can be targeted to reduce seizures. *Nat Med.* 2010;16(4):413-419.
- Fukata M, Yamadevan AS, Abreu MT. Toll-like receptors (TLRs) and Nod-like receptors (NLRs) in inflammatory disorders. *Semin Immunol.* 2009;21(4):242-253.
- Sokolovska A, Becker CE, Ip WKE, et al. Activation of caspase-1 by the NLRP3 inflammasome regulates the NADPH oxidase NOX2 to control phagosome function. *Nat Immunol.* 2013;14(6):543-553.
- Ali MF, Dasari H, Van Keulen VP, et al. Microbial antigens stimulate metalloprotease-7 secretion in human B-lymphocytes using mTOR-dependent and independent pathways. *Sci Rep.* 2017;7(1):3869.
- Li X, Tai HH. Activation of thromboxane A2 receptor (TP) increases the expression of monocyte chemoattractant protein -1 (MCP-1)/

- chemokine (C-C motif) ligand 2 (CCL2) and recruits macrophages to promote invasion of lung cancer cells. *PLoS One*. 2013;8(1):e54073.
21. Astuya A, Rivera A, Vega-Drake K, et al. Study of the ichthyotoxic microalga *Heterosigma akashiwo* by transcriptional activation of sublethal marker Hsp70b in Transwell co-culture assays. *PLoS One*. 2018;13(8):e0201438.
  22. Fedchenko N, Reifenrath J. Different approaches for interpretation and reporting of immunohistochemistry analysis results in the bone tissue – a review. *Diagn Pathol*. 2014;9:221.
  23. Weber A, Wasiliew P, Kracht M. Interleukin-1 (IL-1) pathway. *Sci Signal*. 2010;3(105):cm1.
  24. Cortes-Dericks L, Froment L, Boesch R, Schmid RA, Karoubi G. Cisplatin-resistant cells in malignant pleural mesothelioma cell lines show ALDH(high)CD44(+) phenotype and sphere-forming capacity. *BMC Cancer*. 2014;14:304.
  25. Ghani FI, Yamazaki H, Iwata S, et al. Identification of cancer stem cell markers in human malignant mesothelioma cells. *Biochem Biophys Res Commun*. 2011;404(2):735-742.
  26. Davies S, Beckenkamp A, Buffon A. CD26 a cancer stem cell marker and therapeutic target. *Biomed Pharmacother*. 2015;71:135-138.
  27. Takeda M, Ohe Y, Horinouchi H, et al. Phase I study of YS110, a recombinant humanized monoclonal antibody to CD26, in Japanese patients with advanced malignant pleural mesothelioma. *Lung Cancer*. 2019;137:64-70.
  28. Shi JH, Sun SC. Tumor necrosis factor receptor-associated factor regulation of nuclear factor  $\kappa$ B and mitogen-activated protein kinase pathways. *Front Immunol*. 2018;9:1849.
  29. Tian Y, Kelemen SE, Autieri MV. Inhibition of AIF-1 expression by constitutive siRNA expression reduces macrophage migration, proliferation, and signal transduction initiated by atherogenic stimuli. *Am J Physiol Cell Physiol*. 2006;290(4):C1083-C1091.
  30. Furuya S, Chimed-Ochir O, Takahashi K, David A, Global TJ, Disaster A. Global asbestos disaster. *Int J Environ Res Public Health*. 2018;15(5):1000.
  31. De Meester I, Korom S, Van Damme J, Scharpé S. CD26, let it cut or cut it down. *Immunol Today*. 1999;20(8):367-375.
  32. Havre PA, Abe M, Urasaki Y, Ohnuma K, Morimoto C, Dang NH. The role of CD26/dipeptidyl peptidase IV in cancer. *Front Biosci*. 2008;13:1634-1645.
  33. Pang R, Law WL, Chu ACY, et al. A subpopulation of CD26+ cancer stem cells with metastatic capacity in human colorectal cancer. *Cell Stem Cell*. 2010;6(6):603-615.
  34. Yap TA, Aerts JG, Popat S, Fennell DA. Novel insights into mesothelioma biology and implications for therapy. *Nat Rev Cancer*. 2017;17(8):475-488.
  35. Bronte V, Murray PJ. Understanding local macrophage phenotypes in disease: modulating macrophage function to treat cancer. *Nat Med*. 2015;21(2):117-119.
  36. Pasello G, Zago G, Lunardi F, et al. Malignant pleural mesothelioma immune microenvironment and checkpoint expression: correlation with clinical-pathological features and intratumor heterogeneity over time. *Ann Oncol*. 2018;29(5):1258-1265.
  37. Krysko O, Løve Aaes T, Bachert C, Vandenebeebe P, Krysko DV. Many faces of DAMPs in cancer therapy. *Cell Death Dis*. 2013;4:e631.
  38. Dean M, Fojo T, Bates S. Tumour stem cells and drug resistance. *Nat Rev Cancer*. 2005;5(4):275-284.
  39. Inamoto T, Yamada T, Ohnuma K, et al. Humanized anti-CD26 monoclonal antibody as a treatment for malignant mesothelioma tumors. *Clin Cancer Res*. 2007;13(14):4191-4200.
  40. Angevin E, Isambert N, Trillet-Lenoir V, et al. First-in-human phase 1 of YS110, a monoclonal antibody directed against CD26 in advanced CD26-expressing cancers. *Br J Cancer*. 2017;116(9):1126-1134.
  41. Garlanda C, Dinarello CA, Mantovani A. The interleukin-1 family: back to the future. *Immunity*. 2013;39(6):1003-1018.
  42. Ridker PM, MacFadyen JG, Thuren T, et al. Effect of interleukin-1 $\beta$  inhibition with canakinumab on incident lung cancer in patients with atherosclerosis: exploratory results from a randomised, double-blind, placebo-controlled trial. *Lancet*. 2017;390(10105):1833-1842.
  43. Gordon SR, Maute RL, Dulken BW, et al. PD-1 expression by tumour-associated macrophages inhibits phagocytosis and tumour immunity. *Nature*. 2017;545(7655):495-499.

#### SUPPORTING INFORMATION

Additional supporting information may be found online in the Supporting Information section.

**How to cite this article:** Horio D, Minami T, Kitai H, et al. Tumor-associated macrophage-derived inflammatory cytokine enhances malignant potential of malignant pleural mesothelioma. *Cancer Sci*. 2020;111:2895–2906. <https://doi.org/10.1111/cas.14523>